Climate-driven variation in mosquito density predicts the spatiotemporal dynamics of dengue

Ruiyun Li[a,1,2], Lei Xu[a,b,1], Ottar N. Bjørnstad[c,1], Keke Liu[b,d], Tie Song[e], Aifang Chen[f], Bing Xu[g,3], Qiyong Liu[b,d,3], and Nils C. Stenseth[a,g,3]

[a]Centre for Ecological and Evolutionary Synthesis, Department of Biosciences, University of Oslo, N-0316 Oslo, Norway; [b]State Key Laboratory of Infectious Disease Prevention and Control, Collaborative Innovation Center for Diagnosis and Treatment of Infectious Diseases, National Institute for Communicable Disease Control and Prevention, Chinese Center for Disease Control and Prevention, 102206 Beijing, China; [c]Center for Infectious Disease Dynamics, Pennsylvania State University, University Park, PA 16802; [d]Shandong University Climate Change and Health Center, School of Public Health, Shandong University, Jinan 250012, Shandong, China; [e]Guangdong Provincial Center for Disease Control and Prevention, 511430 Guangzhou, China; [f]Regional Climate Group, Department of Earth Sciences, University of Gothenburg, 40530 Gothenburg, Sweden; and [g]Department of Earth System Science, Tsinghua University, 10084 Beijing, China

Dengue is a climate-sensitive mosquito-borne disease with increasing geographic extent and human incidence. Although the climate–epidemic association and outbreak risks have been assessed using both statistical and mathematical models, local mosquito population dynamics have not been incorporated in a unified predictive framework. Here, we use mosquito surveillance data from 2005 to 2015 in China to integrate a generalized additive model of mosquito dynamics with a susceptible–infected–recovered (SIR) compartmental model of viral transmission to establish a predictive model linking climate and seasonal dengue risk. The findings illustrate that spatiotemporal dynamics of dengue are predictable from the local vector dynamics, which in turn, can be predicted by climate conditions. On the basis of the similar epidemiology and transmission cycles, we believe that this integrated approach and the finer mosquito surveillance data provide a framework that can be extended to predict outbreak risk of other mosquito-borne diseases as well as project dengue risk maps for future climate scenarios.

dengue fever | climate variation | mosquito density | integrated modeling approach

A s one of the most important mosquito-borne diseases in the world, dengue fever is currently affecting almost one-half of the world's population (1). Dengue is a climate-sensitive disease, with prominent effects caused by temperature and precipitation through both direct and indirect pathways (2, 3). For example, temperature determines the extrinsic incubation period directly (4, 5). Additionally, population dynamics of *Aedes aegypti* and *Aedes albopictus*, the most important vectors for viral transmission between humans, are strongly dependent on climate conditions (2). There are four distinct serotypes of dengue virus (1), all of which cocirculate in Asia, Africa, and the Americas. Recovery from infection provides lifelong immunity to each specific serotype but only partial immunity to others (1). Antibody-mediated enhancement during reinfection of heterologous serotypes can cause severe hemorrhagic fever.

Since the first post-World War II dengue outbreak in China in 1978, the affected area has expanded from Hainan and Guangdong Provinces to other coastal and inner regions (6). Recently, unprecedentedly severe dengue outbreaks occurred in China, with 45,230 cases being reported in Guangdong Province in 2014 (3) and around 200 cases in Shandong Province in north China in 2017. The spatiotemporal expansion of dengue incidence (Fig. 1) is an increasing cause of public health concern and a significant economic burden both globally and in China.

Empirical environment–pathogen–host associations have been explored in many studies but are inconsistent among different locations and time periods (2, 7, 8). In addition, global vector distribution and risk prediction cannot be downscaled spatially and temporally without the incorporation of local vector dynamics and their link to environmental conditions (9). Monitoring of local

mosquito abundance on finer spatiotemporal scales is, therefore, of great importance to understand the climate–epidemic interactions and the associated heterogeneities in transmission potential and outbreak risk, which could be used to inform local control strategies and predict future threats. Despite *Aedes* mosquitos being a major threat to human wellbeing, there is a surprising scarcity of time series data on abundance. In 2005–2016, a standardized mosquito monitoring program was carried out by the Chinese Centre for Disease Control and Prevention across 44 major cities at risk for dengue reemergence.

We combine statistical and mathematical approaches to investigate the link between climate and dengue transmission. Generalized additive models (GAMs) have previously proven useful to elucidate the nonlinear statistical relationship between vectors, human incidence, and climate conditions (3). However, mechanistic aspects of transmission have not been incorporated into these statistical analyses. The current challenge is thus to link the statistical models with mechanistic epidemiological models to estimate key epidemiological parameters, such as spatiotemporal variation in the basic reproductive ratio, as well as forecast future outbreak risks in the face of changing environmental conditions (10). We use an integrated modeling approach that links climate-based influences on mosquito abundance to vectored transmission among humans. More precisely, the

---

Significance

Using extensive data on dengue fever and mosquito density, we demonstrate that local weather conditions, through their impact on the variation of mosquito abundance, are a driver of dengue dynamics in China. We believe that this mechanism can be applied to explain dengue dynamics in other places as well. We furthermore conjecture that our integrative approach would be applicable to other vector-borne diseases, such as Zika, malaria, and chikungunya.

Fig. 1. Spatial and temporal distribution of dengue human incidence in 2005–2015. (*A*) Times series of the dengue human incidence in China (on the logarithmic scale) is projected to (*B*) case numbers and distinguished by color according to the magnitude in each city.

long-term mosquito surveillance data from China are incorporated in a generalized additive time series model to establish a predictive climate–mosquito association using

$$M_{i,j} = a_{i,j} + b(Lon_j, Lat_j) + c(T_{i-1,j}) + d(P_{i-1,j}, by = Area) + \varepsilon_{i,j},$$
[1]

where $M_{i,j}$ is the mosquito abundance in month i in city j. The parameter $a_{i,j}$ is the overall intercept, and $b(Lon_j, Lat_j)$ is a two-dimensional smooth function accounting for spatial heterogeneity. The mean temperature and the number of precipitating days in the last month [$c(T_{i-1,j})$ and $d(P_{i-1,j})$, respectively] are used to incorporate 1-mo lag correlation between mosquito density and meteorological variables. *Area* is the categorical factor that classifies cities into north (>32° N), middle (28° N to 32° N), and south (<28° N) China to represent the differing effects of precipitation on mosquito density across areas. The $\varepsilon_{i,j}$ represents model error with an autoregressive structure to account for the serial dependence in time series data.

The climate-driven variation in mosquito density is posited as a proxy for transmission rate of dengue in an epidemiological susceptible–infected–recovered (SIR) model described by the following equations:

$$\frac{dS}{dt} = -\frac{\beta'(t)\widehat{M}SI}{N}$$
[2]

$$\frac{dI}{dt} = \frac{\beta'(t)\widehat{M}SI}{N} - \gamma I$$
[3]

$$\frac{dR}{dt} = \gamma I,$$
[4]

where S, I, and R are the numbers of susceptible, infectious, and recovered humans, respectively. N is human population size, and M is the biweekly mosquito density estimated using the GAM statistical model; $1/\gamma$ is the mean infectious period, and $\beta'(t)$ is the per mosquito vector efficiency. We allow for smooth seasonal variation in $\beta'(t)$ to accommodate factors, such as seasonal variation in mosquito age structure. When incorporated in a mechanistic compartmental model, we find a correspondence between predicted and observed outbreak trajectories of most major dengue outbreaks across multiple years and cities; the analysis reveals important climate-driven variation in dengue's basic reproductive ratio in space and time. We thus clarify the extent to which the synthesis of mosquito surveillance data and an integrated modeling framework can capture and predict dengue human cases. Our findings demonstrate that the long-term city-level mosquito surveillance data are reliable for inferring dengue cases and
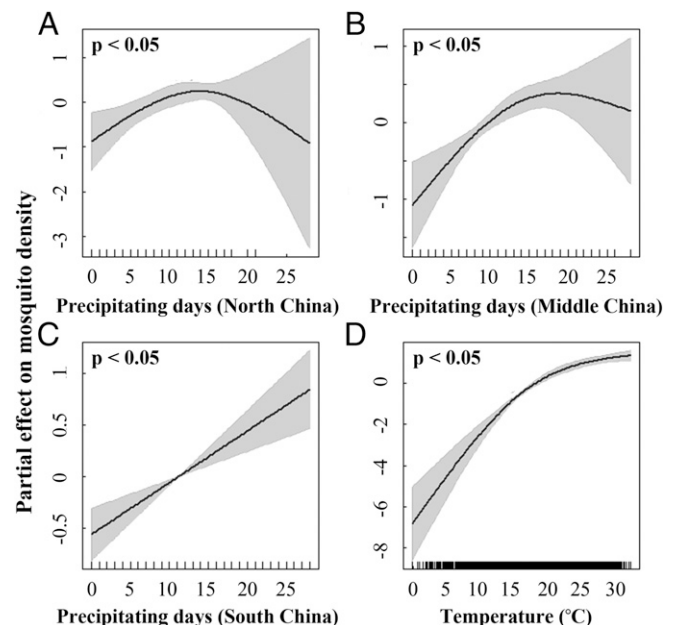
have potential for projecting future risk in the face of a changing environment.

Results

Climate–Mosquito Associations. We found a significant association between mosquito density and local climate conditions in the previous month, with somewhat differing precipitation–abundance associations among the three regions of China (Fig. 2). The precipitation–abundance association is generally increasing in all areas. The nonlinear association in the northern and middle regions indicates that precipitation is of the greatest impact around 15 d/mo ($F_{1.85, 31.8} = 25.89$, $P < 0.05$), whereas the approximately linear relationship ($F_{1, 31.8} = 25.22$, $P < 0.05$) indicates that all precipitation leads to increased mosquito abundance in the southern region. The overall dryer climate in the northern area results in a lower number of precipitating days and hence, a greater uncertainty in estimates of the partial effect of precipitation on mosquito density. We also found a nonlinear but generally increasing association between mean temperature in the previous month and mosquito density ($F_{1.97, 31.8} = 229.09$, $P < 0.05$).

The statistical model captures the dynamics of the observed mosquito abundance across 26 selected cities throughout the 2006–2015 period (*SI Appendix*, Fig. S1) and reveals strong seasonality and geographical variability (*SI Appendix*, Fig. S2). More specifically, there is a general increase in abundance from July to October, reaching the peak magnitude around August. However, the extent of the surge of mosquitos differed among cities, with the most prominent increase in the southern and eastern areas (i.e., Guangdong, Hainan, Zhejiang, and Shandong Provinces). We incorporated biweekly variation in mosquito density during 2005–2015 for the eight representative cities in our mathematical model (*SI Appendix*, Fig. S3).

The 1-mo lag association between local weather condition and mosquito abundance was further validated by the comparison of alternative assumptions. The findings (*SI Appendix*, Table S1) demonstrate that local weather conditions in the contemporary month and 2 mo ago do not have a significant impact on mosquito

Fig. 2. Partial effect from temperature and precipitation on mosquito density. The potential nonlinear effects of the number of precipitating days in (*A*) north, (*B*) middle, and (*C*) south China and (*D*) mean temperature in the previous month on mosquito density are quantified using GAM. Results of the significance test are also shown for each partial effect of climate predictor on mosquito density.
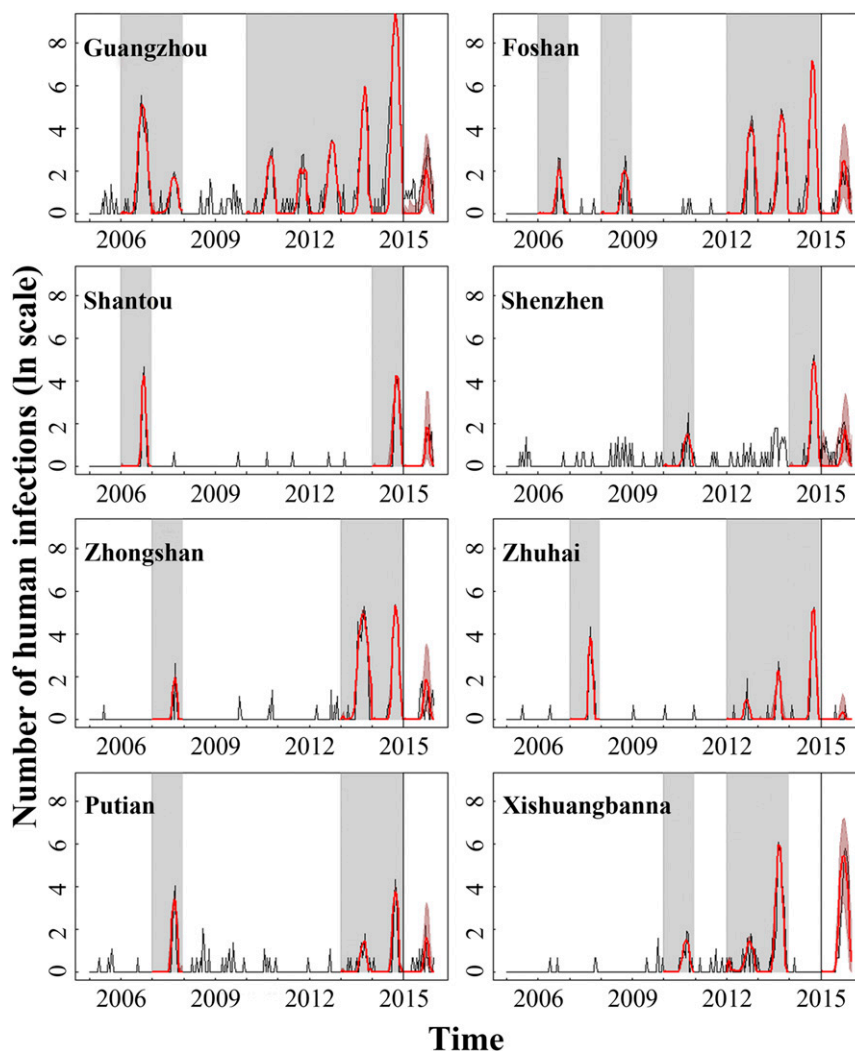
ECOLOGY

density, which verifies the correspondence between mosquito abundance and weather condition in the last month.

Predicting Human Incidence. To link mosquito abundance to human transmission, we assume a seasonal compartmental SIR model for which the transmission rate is driven by vector abundance. The fitted incidence matches the dynamics of observed human cases well (Fig. 3 and *SI Appendix,* Fig. S4). Our climate-driven models thus accurately characterize human risk across a range of magnitudes in different years and cities, including the large outbreak in Guangzhou in 2014. In addition, the inferred annual cycle of epidemic dynamics among most cities is similar in terms of vector efficiency and basic reproductive ratio during the 10-y period. Precisely, the analysis further reveals seasonality in the per mosquito transmission rate, reaching a maximum between the middle of July and late September across most cities (*SI Appendix,* Fig. S5). Notably, seasonal variation in R_0 shows that the epidemic season (when $R_0 > 1$) lasts for 4–5 mo, typically starting in May (9th to 11th biweek) and ending in the middle of September to October (19th to 21st biweek) depending on year and city (Fig. 4). Despite the generally concordant patterns, there is evidence of comparatively higher
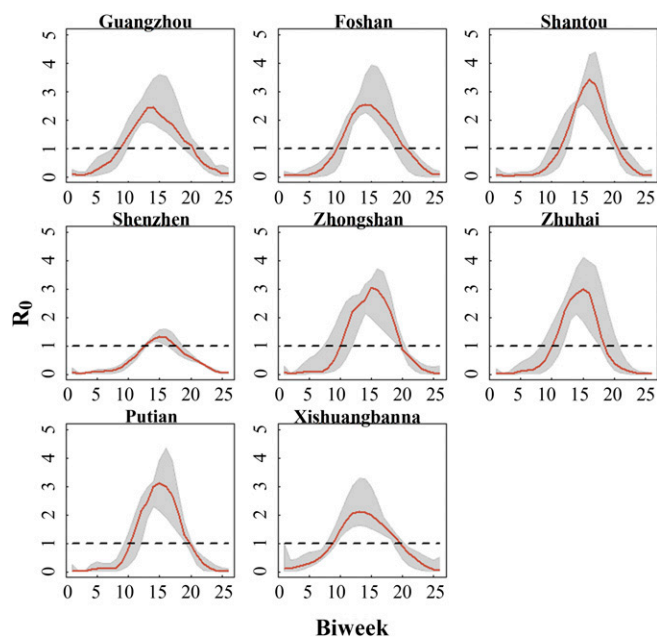
vector efficiency in Shantou and a shorter epidemic period/less probability of widespread transmission in Shenzhen, even when differences in mosquito abundance are accounted for. It is also worth noting that the relative effect of mosquito abundance and vector efficiency in regulating transmission risk is distinct across years and cities (*SI Appendix,* Fig. S6). Specifically, mosquito abundance is the dominant driver of human incidence before 2013 in Guangzhou, Foshan, and Xishuangbanna. Conversely, increase in per mosquito transmission rate seems to drive the increase in risk during 2013–2014. In particular, transmission risk in Guangzhou in 2014 is shaped by significant increase in vector efficiency, indicating a role of factors other than local weather conditions in mediating transmission and inducing that particularly explosive outbreak.

To test our model's ability to perform out-of-sample predictions, we used models trained on the 2005–2014 portion of the data to predict the 2015 outbreaks. There is generally a close match between the predicted and observed dengue cases where the overall trajectory and relative magnitudes of outbreaks in different cities are captured (Fig. 3 and *SI Appendix,* Fig. S4).

The validation of our proposed SIR mechanism that local weather conditions drive dengue dynamics through their impact on mosquito

Fig. 3. Observed and predicted dengue human cases across various cities between 2005–2015. The observed number of human cases in outbreak years (the gray shaded area) during 2005–2014 is used for model simulation and parameter estimation. The model was reinitialized using a plausible range of infectious periods at the beginning of each outbreak year. The median estimates of human cases (red lines) and corresponding confidence intervals (red shaded area) for both simulation and forecasts were compared with observed data (black lines) on the logarithmic scale.

Fig. 4. The dynamics of R_0 during 2005–2014. The median estimates and the corresponding 5th and 95th quantile intervals represent the seasonality of the human-to-human basic reproductive rate in each city in 2005–2014.

abundance with a 1-mo lag was done through comparison with the performance of the alternative hypotheses and mechanisms. Our climate–epidemic model has a better root mean square error (RMSE) than the null model, where mosquito abundance was not incorporated (*SI Appendix*, Fig. S7). This finding demonstrates that a "vector-free" model with a simple spline-fitted transmission rate cannot accurately capture the complex interactions at the climate–mosquito–virus interface. Therefore, an alternative hypothesis that assumes a direct impact of climate factors on transmission rate does not perform well in characterizing dengue transmissions. Additionally, statistical testing verifies the significant outperformance of the time-dependent vector model over the alternative constant vector efficiency (*SI Appendix*, Table S2). That is, seasonal variation of mosquito abundance alone cannot fully characterize the mosquito–human interactions as well, which is presumably due to the seasonality in human/mosquito activity patterns as well as shifts in vector age structure (11).

Discussion

In our study, long-term mosquito surveillance data from many Chinese cities are incorporated in the analysis of a vector-borne human infection. The seasonality of R_0 generally follows the climate-driven dynamics of mosquito abundance, which remain at a higher level from May/June to September/October. This finding clarifies how local mosquito abundance combined with various other seasonal factors may cause explosive dengue risk to humans. Our findings further highlight the importance of city-level mosquito surveillance data integrated with a synthetic mathematical framework to successfully predict dengue risk.

Our integrated modeling approach improves inference on dengue transmission at the climate–epidemic interface. Moreover, the statistical model allows prediction of the temporal dynamics of mosquito abundance in locations where no or only partial monitoring is available. The improved mosquito estimates not only make up for the surveillance bias but also, allow prediction of seasonal dynamics of human cases when used to force an SIR compartmental model. The seasonality in transmission rate is likely to reflect the effects of multiple factors and complex interactions at the mosquito–human interface that impact dengue risk through heterogeneous

mechanisms at various spatial–temporal scales (12). More specifically, we found that local weather conditions directly regulate adult mosquito density through variation in precipitation and temperature with a roughly 1-mo lag. However, effects of other climate and nonclimate factors on dengue risk may be exerted over longer periods of time and across other spatial scales. For example, previous studies have documented a significant coherence between the interannual dynamics of El Niño–Southern Oscillation-related climate anomalies and dengue incidence in countries, such as Thailand, Mexico, and some island nations of the South Pacific (13–16). Some nonclimatic drivers, such as human movements, have also been documented to mediate exposure risk to vectors, dengue transmission rates, and spatial patterns at finer scales (17, 18). The validation of our proposed modeling framework further indicates that the complex interactions underlying dengue transmission can only be accurately characterized by considering mosquito abundance and seasonality in vector efficiency. The latter plausibly comes about because of the extrinsic incubation period as well as adult mosquito age structure variations throughout the year. This model's outperformance in inferring dengue risk may partially be explained by the multiple ways that climate influences transmission. Put another way, by independently simulating the nonlinear variation in mosquito abundance and vector efficiency, the multiple sources of seasonality are better characterized, leading to better inference on human risk. In contrast, alternative models that assume either a direct climate impact on transmission or a constant vector efficiency are not adequate for predicting the interactions at the climate–vector–dengue interface. Notably, the outperformance of this proposed climate–mosquito–epidemic mechanism in driving dengue dynamics should not be interpreted as the consistent pathway but should be verified spanning different transmission settings and spatiotemporal scales.

Some limitations should be taken into consideration when interpreting our studies. Themed around climate–mosquito associations, our inference on dengue risk should be interpreted as an outbreak potential caused by local climate and mosquito conditions. This is because current mosquito control strategies are increasingly effective in reducing the risk of human infections (1), particularly after the occurrence of the big outbreak in Guangzhou in 2014. Such controls will alter the suitable transmission condition and potential transmission bounds set by climate alone. The human risk is also likely underestimated, because asymptomatic infections are not included in our analysis. Therefore, additional research is needed to quantify the relative contribution of other determinants of risk in modulating transmission condition and human risk in each city to make more accurate forecasts across different geographical locales. Additionally, potential bias in mosquito surveillance may affect the spatiotemporal surveillance of mosquito abundance. The large variation in mosquito abundance within cities reflects both the seasonality of the mosquito population and the role of mosquito surveillance in guiding control strategies. Specifically, seasonal dynamics of mosquito density follow the fluctuation of local climate conditions, with peak abundance in the summer. The heterogeneous control strategies across cities and specific surveillance sites may lead to anomalous fluctuations in mosquito density (*SI Appendix*, Fig. S2). Generally, southern cities are of higher risk and hence, have more intensified prevention and control routines, whereas northern cities tend to have moderate controls only after the occurrence of outbreaks. Likewise, mosquito abundance in newly selected surveillance sites may be higher due to a lack of previous interventions. Moreover, the selection of 1-mo lag in weather–abundance association is dependent on the mosquito lifecycle. In light of the lower proportion of explained deviation and a higher generalized cross-validation criteria (GCV) value compared with the 1-mo lag model, the additional incorporation of meteorological factors in contemporary month and 2 mo ago does not have significant impact on mosquito abundance.

With this study, we have demonstrated that variation in local climate conditions, through their impact on mosquito abundance, provides a plausible mechanism for explaining the observed dengue dynamics in China—a mechanism that we have reason to assume is a general one. Mosquito surveillance on a finer scale and local weather conditions are thus of the utmost importance for predicting outbreak risks and optimizing local control and prevention strategies as well as projecting outbreak risk into the future.

Methods

Dengue Human Cases. Case-level records of dengue human data from January 2005 to December 2015 in China were obtained from the China National Notifiable Disease Surveillance System. The associated information of each case, including age, sex, occupation, date of onset, and description about travel or contact history, was also collected. Biweekly human cases were summarized for the mathematical modeling analysis.

Mosquito Surveillance Data. Mosquito surveillance of both *A. aegypti* and *A. albopictus* from January 2005 to December 2015 was implemented by the Chinese Center for Disease Control and Prevention using light traps. The selection of representative trap sites was based on local mosquito breeding ecosystems, epidemic areas, and feasibility of surveillance, and sites included households, residential areas, parks, construction sites, and hospitals. Specifically, a light trap was placed at the sheltered site away from light and ~1.5 m above the ground. The light was on, and surveillance was performed at night from 1 h before sunset to 1 h after sunrise. Traps were collected daily, and mosquitoes were collected for subsequent analyses, including the identification of species, sexing, and total count. Since *A. aegypti* is the dominant species in most cities (*SI Appendix*, Table S3), we aggregated the number of the two species, with the assumption of similar viral transmission ability of the two. The monthly number of mosquitoes was transformed to monthly mosquito density (unit: number of mosquitoes per trap). The number of monitored cities increased from 32 to 44 during 2006–2015, among which the observed mosquito density in 26 cities was greater than zero. These were used for additional statistical modeling (*SI Appendix*, Fig. S8).

Local Meteorological Variables. Daily mean temperature and precipitation data during 2005–2015 were obtained from the China Meteorological Data Sharing Service System (data.cma.cn; last accessed January 29, 2018). The obtained meteorological dataset was processed into monthly mean temperature and the number of precipitating days (number of days with precipitation over 1 mm/d) (19) to reconstruct the mosquito density in the statistical analysis.

Statistical Analysis. GAMs with a negative binomial distribution and autoregressive error term were used to study the association between local weather conditions and mosquito population dynamics according to Eq. **1**. The analyses were implemented using the mgcv package in R. Based on the lifecycle of the mosquito, we posited a 1-mo lag between adult mosquito abundance and meteorological variables. That is, we assumed that the adult mosquito density is related with a time lag to the premature stages, which are directly influenced by meteorological factors. Therefore, the mean temperature and the number of precipitating days in the last month [i.e., $c(T_{i-1, j})$ and $d(P_{i-1, j}, by = Area)$] were used to predict mosquito density in the current month. In light of the differential impact of precipitation in different climate regions in China (20–22), a smooth function with a categorical indicator (i.e., *Area*) was chosen for precipitation to allow for a heterogeneous precipitation–abundance association. Specifically, 26 mosquito surveillance sites were located in the east monsoon area where regional climate was greatly influenced by precipitation and temperature, with the strongest seasonality in the middle and lower reaches of the Yangtze River (28° N to 32° N). Therefore, we assigned surveillance sites to three different climate subareas: the north (>32° N), middle (28° N to 32° N), and south (<28° N) China.

We first calibrated the model and obtained empirical climate–mosquito associations using both monthly mosquito density and meteorological data at 26 surveillance sites during 2006–2015. This association was then interpolated to get the biweekly mosquito estimates for the period of 2005–2015, which were sequentially used as the proxy of transmission rate among humans in the mathematical model (see below). To further validate the assumption of a 1-mo lag in weather–abundance association, model performance with alternative assumptions (i.e., mosquito abundance is correlated to the weather condition in the contemporary month or the last 2 mo) was evaluated and compared using the GCV. The alternatives provided weaker fits.

The epidemical SIR model used for this study simulates dengue transmission among humans. The model is described by the SIR equations (Eqs. **2–4**).

The mean infectious period, $1/\gamma$, was taken as a random constant from the uniform distribution of 14–18 d as the extrinsic incubation period and the average intrinsic incubation periods 8–12 and 6 d. $\beta'(t)$, the per mosquito transmission rate or the vector efficiency, is the time-dependent scaling factor linking the estimated mosquito density with transmission among humans, $\beta(t)$. More specifically, our modeling framework was implemented with the assumption that the variation of mosquito density over time is highly linked to and can be used as a proxy for the dynamics of transmission among humans. Hence, the transmission rate among humans and human-to-human basic reproductive ratio are calculated as $\beta(t) = \beta'(t)\hat{M}$ and $R_0 = \beta(t)M/\gamma$, respectively. On the basis of the complex interactions at the mosquito–human interface, we used a spline function with three degrees of freedom to estimate the seasonality in vector efficiency, $\beta'(t)$.

The numbers of human cases in outbreak years (or years with prominent magnitude of human cases) during 2005–2014 in eight representative cities (*SI Appendix*, Fig. S9) were selected for SIR model simulation and parameter estimation. With the assumption of a homogeneous susceptibility in the entire population and no underreporting of cases, we reinitialized the model 500 times with different γ values at the beginning of each outbreak year to simulate human incidence. The median estimates of all simulations using the varying γ values are presented. Based on the similarity in local biological and ecological conditions cross-years, dynamics of vector efficiency in 2015 were assumed to follow the general dynamic pattern of those during the previous outbreak years in each city. Therefore, the 10-y averaged dynamics of $\beta'(t)$ obtained from model simulation and estimated mosquito abundance were used to forecast human dengue cases in 2015.

The performance of the SIR model was quantified by the root mean squared error. Additionally, the relative effect of mosquito density and vector efficiency on dengue risk was evaluated by the correlation between the fluctuation of R_0, mosquito abundance, and vector efficiency. Precisely, 10-y averaged values of R_0, mosquito abundance, and efficiency were subtracted to estimate the fluctuation at each biweek relative to the long-term dynamic pattern in a city. The relative contribution of the fluctuation of mosquito abundance and efficiency was subsequently identified by univariate and multivariate correlation analyses. To validate the proposed mechanism that local weather conditions drive dengue dynamics through their impact on mosquito abundance, we further compared our model with two alternative models—one assuming a direct link between weather and dengue and the other assuming no seasonality in vector competence (constant β'). Both alternative models had poorer performance according to their RMSEs.

Data Availability. Daily mean temperature and precipitation data are available from the China Meteorological Data Sharing Service System (data.cma. cn). The dengue human data and mosquito surveillance data are available from the corresponding authors on request. Requests for materials should be addressed to B.X., Q.L., or N.C.S.

1. WHO (2017) Dengue and serve dengue. Available at https://www.who.int/en/news-room/fact-sheets/detail/dengue-and-severe-dengue. Accessed January 29, 2018.
2. Morin CW, Comrie AC, Ernst K (2013) Climate and dengue transmission: Evidence and implications. *Environ Health Perspect* 121:1264–1272.
3. Xu L, et al. (2017) Climate variation drives dengue dynamics. *Proc Natl Acad Sci USA* 114:113–118.
4. McLean DM, et al. (1974) Vector capability of Aedes aegypti mosquitoes for California encephalitis and dengue viruses at various temperatures. *Can J Microbiol* 20:255–262.
5. Watts DM, Burke DS, Harrison BA, Whitmire RE, Nisalak A (1987) Effect of temperature on the vector efficiency of Aedes aegypti for dengue 2 virus. *Am J Trop Med Hyg* 36:143–152.
6. Lai S, et al. (2015) The changing epidemiology of dengue in China, 1990-2014: A descriptive analysis of 25 years of nationwide surveillance data. *BMC Med* 13:100.
7. Johansson MA, Cummings DAT, Glass GE (2009) Multiyear climate variability and dengue–El Niño southern oscillation, weather, and dengue incidence in Puerto Rico, Mexico, and Thailand: A longitudinal data analysis. *PLoS Med* 6:e1000168.
8. Johansson MA, Dominici F, Glass GE (2009) Local and global effects of climate on dengue transmission in Puerto Rico. *PLoS Negl Trop Dis* 3:e382.

9. Messina JP, et al. (2015) The many projected futures of dengue. *Nat Rev Microbiol* 13: 230–239.
10. Beatty M, et al.; WHO-VMI Dengue Vaccine Modeling Group (2012) Assessing the potential of a candidate dengue vaccine with mathematical modeling. *PLoS Negl Trop Dis* 6:e1450.
11. Smith DL, McKenzie FE (2004) Statics and dynamics of malaria infection in Anopheles mosquitoes. *Malar J* 3:13.
12. Lafferty KD (2009) The ecology of climate change and infectious diseases. *Ecology* 90: 888–900.
13. Brunkard JM, Cifuentes E, Rothenberg SJ (2008) Assessing the roles of temperature, precipitation, and ENSO in dengue re-emergence on the Texas-Mexico border region. *Salud Publica Mex* 50:227–234.
14. Cazelles B, Chavez M, McMichael AJ, Hales S (2005) Nonstationary influence of El Niño on the synchronous dengue epidemics in Thailand. *PLoS Med* 2:e106.
15. Hales S, Weinstein P, Souares Y, Woodward A (1999) El Niño and the dynamics of vectorborne disease transmission. *Environ Health Perspect* 107:99–102.
16. Gagnon AS, Bush ABG, Smoyer-Tomic KE (2001) Dengue epidemics and the El Niño Southern Oscillation. *Clim Res* 19:35–43.
17. Stoddard ST, et al. (2013) House-to-house human movement drives dengue virus transmission. *Proc Natl Acad Sci USA* 110:994–999.
18. Stoddard ST, et al. (2009) The role of human movement in the transmission of vector-borne pathogens. *PLoS Negl Trop Dis* 3:e481.
19. Dai A (2006) Precipitation characteristics in eighteen coupled climate models. *J Clim* 19:4605–4630.
20. Zhang R, Wu B, Han J, Zuo Z (2013) Effects on summer monsoon and rainfall change over China due to Eurasian snow cover and ocean thermal conditions. *Climate Change—Realities, Impacts over Ice Cap, Sea Level and Risks*, ed Singh BR (InTech, Rijeka, Croatia), pp 227–250.
21. Ding R, Ha K, Li J (2010) Interdecadal shift in the relationship between the East Asian summer monsoon and the tropical Indian Ocean. *Clim Dyn* 34:1059–1071.
22. Qian W, Ding T, Hu H, Lin X, Qin A (2009) An overview of dry-wet climate variability among monsoon-westerly regions and the monsoon northernmost marginal active zone in China. *Adv Atmos Sci* 26:630–641.

ECOLOGY